LETTER

Transparency in graphene mediated evaporation

2D Materials

LETTER

Transparency in graphene mediated evaporation

Yongfeng Huang[1,2], Jun Lu[1,2] and Sheng Meng[1,2,3]

[1] Beijing National Laboratory for Condensed Matter Physics and Institute of Physics, Chinese Academy of Sciences, Beijing 100190, People's Republic of China
[2] Collaborative Innovation Center of Quantum Matter, Beijing 100190, People's Republic of China
[3] Author to whom any correspondence should be addressed.

E-mail: smeng@iphy.ac.cn

RECEIVED
4 March 2018

REVISED
17 May 2018

ACCEPTED FOR PUBLICATION
4 June 2018

PUBLISHED
13 July 2018

Keywords: water-substrate interaction, wetting, contact angle, molecular dynamics, evaporation

Supplementary material for this article is available online

Abstract

Droplet evaporation is a ubiquitous phenomenon with numerous applications. It plays a pivotal role in life and industry since it concerns heat transfer in high efficiency to reach a desired temperature. However, to rationally mediate evaporation has always been a significant challenge. Here by studying the interactions of water molecules with graphene-covered substrate, we propose that graphene could effectively affect water evaporation rate by changing the length of contact line. More importantly, evaporation per length of contact line before and after graphene coverage shows negligible change, suggesting graphene is transparent for evaporation (per unit contact length). Molecular dynamics simulations confirm experimental findings and indicate that principal evaporation events take place via single-molecule desorption at the contact line.

Introduction

Evaporation of water droplet is a ubiquitous and complicated phenomenon occurring almost everywhere and plays a pivotal role in nature and industry. For animals and plants, evaporation transfers heat away to prevent catastrophic warming up of body, as well as to assist water transport into leaves. Water droplet evaporation also functions vitally in various environmental circumstances including coffee-ring pattern, self-assembly, vapor-mediated sensing, energy harvesting and emulsification [1–12]. With the ubiquity and importance, evaporation has attracted considerable scientific interests calling for a fundamental understanding.

Obtaining deep insights into evaporation mechanism in various circumstances is of vital importance to develop new methods controlling evaporation losses rationally. During past decades, water evaporation has been intensely studied and significant progresses have been achieved [13–25]. In order to depict the evolution of droplet shape during evaporation, two regimes have been proposed: constant contact angle (CCA) regime and constant contact line with a fixed circular diameter, or simply constant contact diameter (CCD) regime [13]. CCA regime describes evaporation process where contact angle of water droplet remains constant but contact area decreases, while in CCD regime contact diameter remains constant but contact angle decreases. Almost all cases of droplet evaporation fall in one of these two regimes.

Previous studies revealed that intrinsic properties of the substrate, especially the wetting states, affect greatly the evaporation of water droplet [18, 26–35]. It was found phenomenologically very strong evaporation takes place at the contact line [1, 16], whose exact dynamics at the molecular scale remain yet unexplained. Graphene has become a hotspot of research in virtue of its extraordinary electronic and mechanical properties [36–38]. The effects of graphene on wetting have attracted tremendous attentions [39–43]. Rafiee *et al* [39] and Raj *et al* [40] found graphene is wetting transparent, namely, the presence of single-layer graphene does not change the wetting angle of the underlying substrate. However, Shih *et al* [41, 42] reported contradictory results that graphene strikingly changes the wetting states of droplet as graphene increases water contact angle from 21° on silica to 40°. There are intensive debates on whether graphene alters the wetting state of a substrate in literature. Consequently, similar to the case of water wetting, it is an interesting open question whether graphene would significantly affect the evaporation of water droplet.

Here we study the evaporation behavior of water droplet on various substrates and their graphene-covered counterparts both experimentally and

theoretically. Graphene suppresses the evaporation rate of droplets by ~20% as it changes the wetting states of droplet on substrates. However, the mean evaporation rate per contact length/diameter (mean contact-diameter evaporation, *MCE*) remains unchanged. For all substrates investigated here, the difference in *MCE* before and after graphene coating is less than 5%, demonstrating graphene is transparent for *MCE*. Molecular dynamics (MD) simulations reproduce experimental findings regarding the evaporation transparency of graphene. Molecular scale analysis suggests that droplet evaporation takes place dominantly at the contact line via single-molecule desorption events. This study sheds light on atomistic mechanism of graphene-mediated evaporation, and is vital towards evaporation control for heat transfer, printing, and self-assembly applications.

Evaporation transparency at the contact line

We study water droplet evaporation on hydrophilic $SrTiO_3$ (STO) (1 1 1), GaP (1 1 1), glass, silicon (Si) (1 0 0) as well as hydrophobic polydimethylsiloxane (PDMS), and graphene-covered counterparts. Graphene is synthesized on copper foil by chemical vapor deposition and then transferred onto the substrates using bubbling transfer method [44, 45] (see supporting information (stacks.iop.org/TDM/5/041001/mmedia)). Optical microscope and Raman spectrum are employed to characterize the transferred large-area graphene with size $1 \times 1\,cm^2$ in figure 1(a). Graphene in the present work is single-layer with high quality, which is confirmed by Raman spectrum (inset of figure 1(a)) [46]. De-ionized water is used for droplet evaporation experiments.

We firstly measure the contact angle of water droplets on these substrates and graphene-covered counterparts (gr/substrates). Side-view images of droplets on Si and gr/Si are displayed in figure 1(b), showing obvious difference with graphene coating. Graphene increases contact angle on hydrophilic substrates. For example, contact angle increases from 36° on STO to 72° on gr/STO. However, on PDMS contact angle decreases from 103° to 92° on gr/PDMS. The result that graphene increases the contact angle on hydrophilic substrates but decreases the contact angle on hydrophobic PDMS, is in good consistency with Shih *et al* [41, 42].

Owing to the wetting states modulated by graphene, the same-volume water droplets possess different contact diameters. On hydrophilic substrates, the contact diameter becomes smaller since graphene increases the contact angle. For example, the contact diameter is 4.00 mm on GaP while 3.14 mm on gr/GaP. On the contrary, contact diameter increases from 2.38 mm on PDMS to 2.65 mm on gr/PDMS.

We next study the evaporation rate of water droplets on these substrates. The initial mass of the droplets is about 4.5 mg. All measurements are performed in the same ambient atmosphere (relative humidity: 52% ± 4% and temperature: 28.0 °C ± 0.5 °C) with graphene coating as the only variant. Schematic of the experimental setup is displayed in figure 2(a).

Evaporation stages are clearly seen by monitoring the evolution of contact diameter and contact angle during evaporation process shown in figure 2(b). Evaporation occurs firstly in the CCD-stage with CCD as marked by dark shadow area. Evaporation in this stage appears on all substrates but with different durations. After that, CCA-stage evaporation follows on glass, Si, PDMS and gr/PDMS, but not obviously on other substrates. Effects of different substrates on evaporation behavior will not be discussed here.

Mass variation with respect to evaporation time is recorded in upper panels of figure 3. We notice it is reasonable to link mass with contact diameter rather than with surface (figures 3 and S2). We define mean contact-diameter mass (*MCM*) to represent mass per unit length of the contact diameter/line (the two differing by a factor of π). We define evaporation rate u and mean contact-diameter evaporation (*MCE*) v as:

$$u = \frac{dm}{dt}, \tag{1}$$

$$v = \frac{d}{dt}\left(\frac{m}{D_c}\right), \tag{2}$$

where m, t *and* D_c represent the mass, time and contact diameter respectively. In equation (2), $\frac{m}{D_c}$ is the *MCM*. Both *MCM* and *MCE* are an average with the length of contact line. We obtain u and v by linear fitting of the experimental data in figure 3, since the mass and *MCM* vary as a function of time almost in the linear form.

In the final stage of evaporation process, accurate measurements of the contact angle and contact diameter are difficult due to irregular shape of the droplet. The chemical inhomogeneity, structure variation of the substrate, and temperature all affect evaporation, while the measurement of mass is more reliable since it is not related with the droplet shape. Therefore, data for longer time are collected in figure 3.

Evaporation rate on hydrophilic substrates is decelerated while on hydrophobic PDMS is accelerated after graphene coating (upper panels of figure 3 and table S1). The most conspicuous change occurs on GaP, where evaporation is decelerated by as much as 17.63%. Evaporation rate is accelerated by 6.85% on PDMS. The findings imply that single-layer graphene strikingly affects evaporation rate of droplets on a solid surface.

However, the evaporation rate per contact line (v) remains unchanged after graphene coating (bottom panels of figure 3). Table 1 lists the values of *MCE* on different substrates and how much it is changed by graphene coating, ranging from 0.87% to 4.17%. Graphene does not change evaporation rate per contact

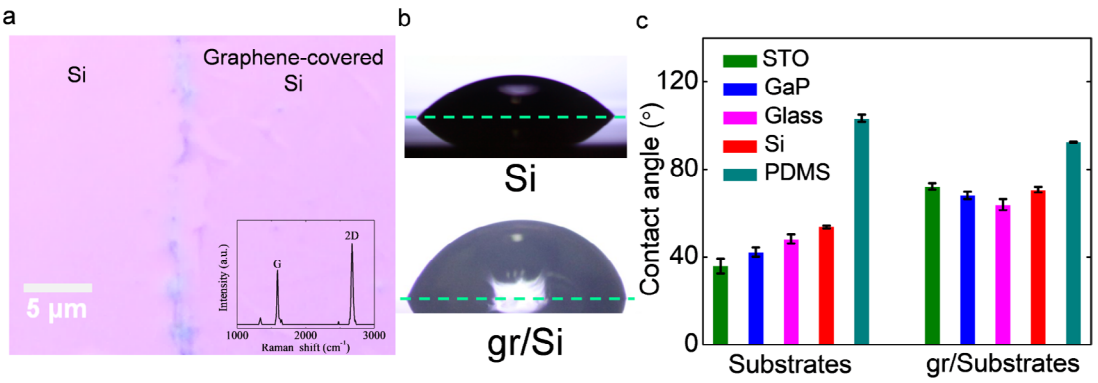

Figure 1. Characterization of graphene and wetting state. (a) Optical image of the single-layered graphene on Si. Color of the graphene-covered Si on the right is a darker than that of Si on the left. Inset: Raman spectrum confirming the high quality of graphene. (b) Side-view of water droplet on Si and on graphene-covered Si (gr/Si). The green dot line is the base line for contact angle measurement in our experiments, representing the water-solid interface. The spherical part above the line is water droplet while the other part below the line is substrate (Si or gr/Si). (c) Contact angle of water droplets on STO, GaP, glass, Si, PDMS and their graphene-covered counterparts.

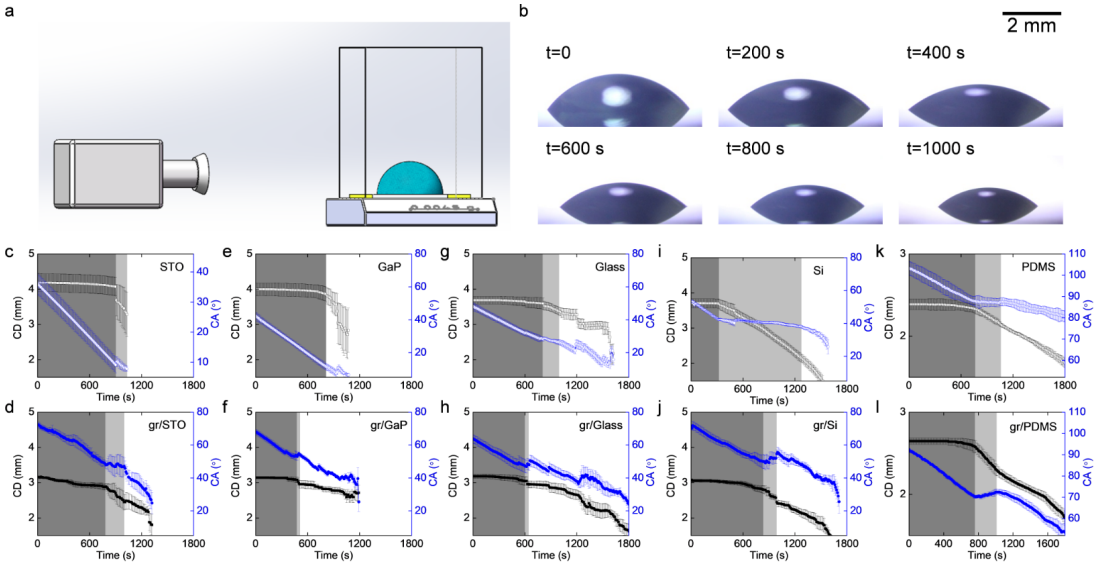

Figure 2. Experimental setup and the process of droplet evaporation. (a) Schematic of our experimental setup. Camera records side-view of water droplet on substrate, placed in digital balance enclosed by a chamber with a size of 14 cm × 17 cm × 22 cm. (b) Side-view of droplet profile on Si as a function of time on during evaporation (scale bar: 2 mm). Contact diameter (CD) and contact angle (CA) changes in the evaporation process on (c) STO, (d) gr/STO, (e) GaP, (f) gr/GaP, (g) glass, (h) gr/glass, (i) Si, (j) gr/Si, (k) PDMS and (l) gr/PDMS.

length, demonstrating graphene is transparent in terms of *MCE* and mediates total evaporation rate by changing the wetting state of water droplet on a substrate.

Atomistic mechanism

To understand the experimental findings, we use MD simulations to study evaporation of water droplet at the atomic scale as previously used [30, 47–50]. The simulations are performed by Large-scale Atomic/Molecular Massively Parallel Simulator (Lammps) [51]. We place a wall above the water droplet to absorb water molecules that escape from the mother-droplet [52, 53] (see Methods for details). Snapshots in figure 4(a) show the simulated evaporation process with mother-droplet clearly seen at different times. Figure 4(b) shows that the contact diameter of the droplet decreases from 8.5 nm on Si to 7.0 nm on gr/Si, which is consistent with our experimental results on wetting states.

From figure 3 it seems that our major conclusion that graphene is transparent for evaporation per contact line length is valid for both CCD and CCA regimes. We note our model of *MCE* is built without any bias on the evaporation regime, and thus should apply for different evaporation regimes including both CCD and CCA. We focus on the evaporation in the CCD regime, since in experiments the majority of evaporation-induced mass loss takes place in the CCD mode. In both experiments and MD simulations,

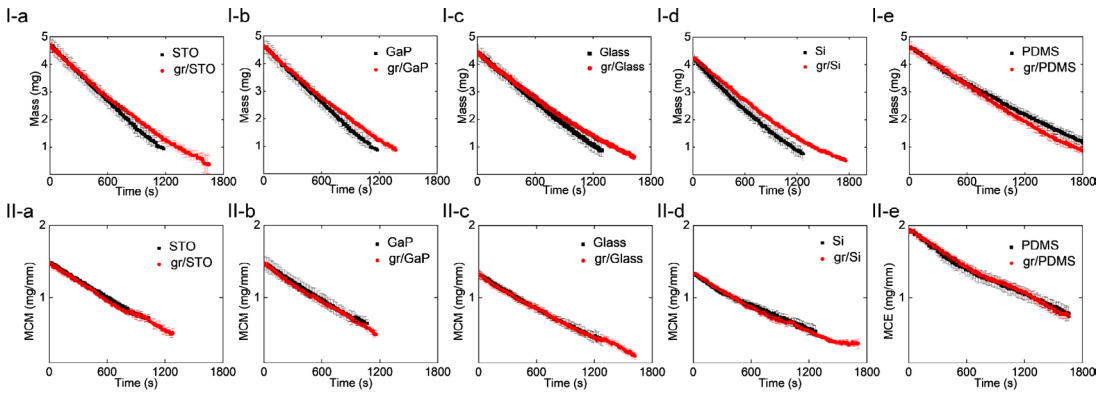

Figure 3. Comparison of mass, mass per surface area and mean contact-diameter mass (*MCM*). I: Mass changes of water droplets on (a) STO and gr/STO; (b) GaP and gr/GaP; (c) glass and gr/glass; (d) Si and gr/Si; (e) PDMS and gr/PDMS. II: *MCM* for droplets on (a) STO and gr/STO; (b) GaP and gr/GaP; (c) glass and gr/glass; (d) Si and gr/Si; (e) PDMS and gr/PDMS. Graphene caused no changes on *MCM* as a function of time.

Table 1. Mean contact-diameter evaporation (*MCE*) rate on different substrates (The difference is defined as *MCE* changes due to graphene coating.)

	MCE (10^{-4} mg/mm/s)		
	Bare	gr-covered	Difference (%)
STO	7.83	7.59	−3.07
GaP	8.03	7.96	−0.87
Glass	7.18	7.07	−1.53
Si	5.99	5.74	−4.17
PDMS	8.79	8.49	−3.41

evaporation occurs firstly in the CCD regime where the contact diameter can be well defined, while in CCA mode identifying the precise contact diameter is challenging.

We replace the mass and *MCM* of droplet by the number of water molecules *N* and mean contact-diameter number (*MCN*). The number of water molecules *N* on the two substrates decreases in apparently disparate ways: *N* on Si decreases faster than that on gr/Si (figure 4(c)). On Si, 432 water molecules evaporate away while on gr/Si 394 molecules evaporate away. Evaporation rate is 9% smaller in the presence of graphene, close to the experimental value of 12%.

Apparently the temporal evolution of droplet mass in MD simulations shows a convex profile, at variance with that in experiments. We note that in the initial stages of evaporation both experiments and MD simulations follow a nearly linear loss in droplet mass as a function of time, showing a generally good agreement. It is worth to point out that the length scales in the experiments (~5 mm) and MD simulations (~5 nm) differ by six orders of magnitude. Consequently, the large thermal fluctuations in nanoscale simulations would accelerate the evaporation rate during droplet evaporation. Moreover, in macroscopic experiment due to the presence of charged defects and non-homogeneity of the substrate, the pinning effects of water droplet are unavoidable in the later stage of evaporation, which slow down the droplet evaporation rate. Such pinning effects and the presence of defects are not considered in MD simulations. However, the discussion on the precise evaporation model is not the focus here; instead, we focus on the comparison of water evaporation with and without graphene. We can see that the difference in evaporation rate per contact line due to the presence of graphene is negligible in figure 4(d), which is in good correspondence with the experimental results.

Evaporation transparency results from the fact that evaporation of the droplet takes place primarily at the contact line via single-molecule desorption processes. A water molecule first diffuses from the bulk to the region nearby the droplet surface; therefore, molecular distribution in the region nearby the droplet surface is crucial. We show the trajectory of water molecules by superimposing 500 snapshots in the 3 ns simulation of evaporation on Si in figure 5(a). Molecules possessing at least one neighboring molecule with a distance no more than 0.35 nm are shown, representing water molecules in bulk and those in the transition state from the liquid to gas phase. The number density of water molecules is much larger at the contact line than that from the liquid surface. Besides, we also observe that water molecules form a thin film on the substrate around the mother-droplet. The precursor water film at the outer edge of the droplet contact line will significantly reduce water desorption barrier therein, compared to other surfaces of the droplet, favoring water evaporation. This suggests the dominant evaporation process occurs with water molecules diffusing along the substrate surface, assisted by the surface potential, and desorbing from the substrate, yielding the largest evaporation rate at the contact line. We further divide the region nearby the droplet into several layers parallel to the substrate and thickness of each layer is 0.35 nm. Radius of each layer is 0.5 nm greater than the radius of liquid part in the same layer. We use number of water molecules divided by the volume of each layer averaged over 500 snapshots to represent molecular

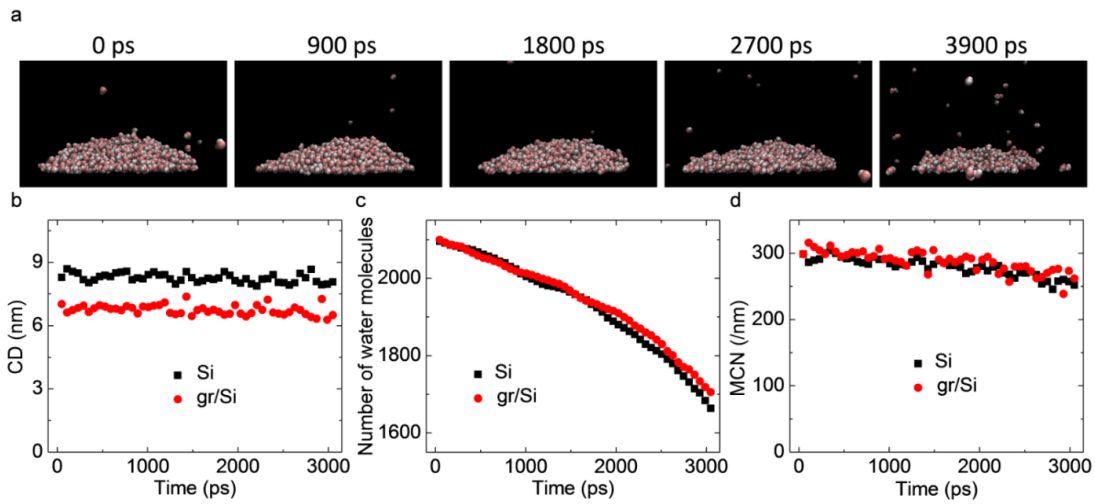

Figure 4. Evaporation by MD simulations. (a) Snapshot sequences of the main evaporation process with the clear mother-droplet. (b) Contact diameter of the droplet remains almost constant during simulation. (c) Number of water molecules in the droplet decreases as a function of time. (d) *MCN* of water molecules decreases in almost the same slope with time on both substrates.

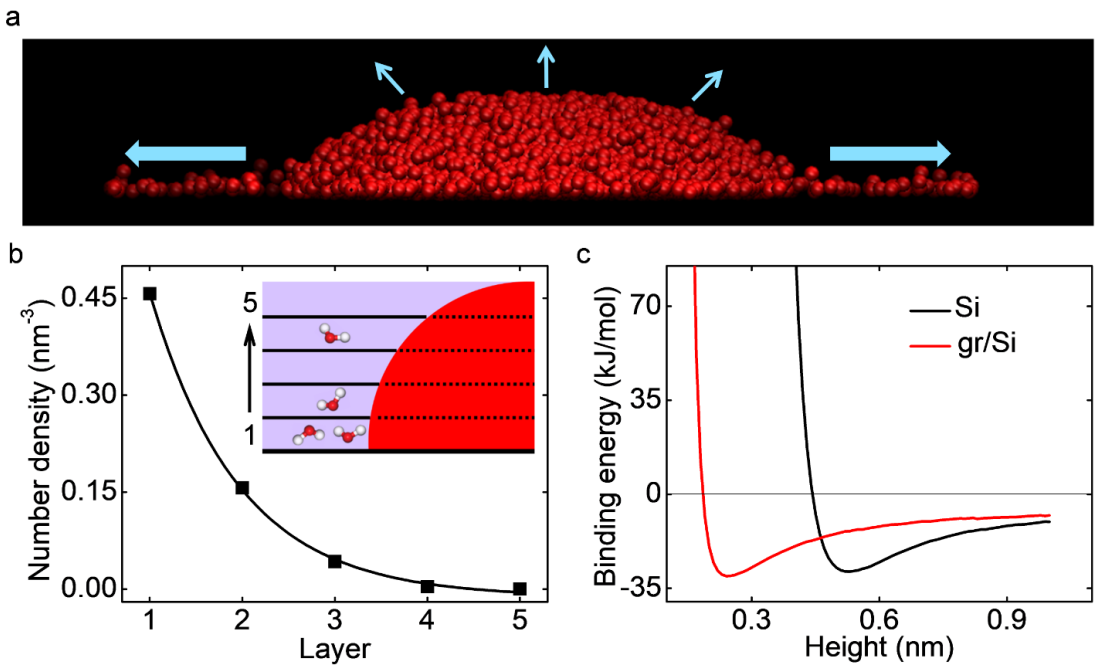

Figure 5. Evaporation at molecular scale. (a) Transition state shows the trajectory of molecules from liquid to gas. (b) Molecular distribution of the transition states nearby the droplet surface. The number density is averaged over 500 snapshots in each layer. Insert: Layer number starts from 1 to 5. (c) The binding energy distribution as a function of the distance on Si and gr/Si.

distribution. It has a maximum at the contact line, and deceases exponentially as the layer going away from the substrate. The distribution suggests that evaporation events dominantly take place at the contact line and decreases rapidly in the exponential form (figure 5(b)).

Evaporation rate at the contact line would be the same with and without graphene coating because graphene has negligible effects on the binding energy of a single water molecule. Take the Si substrate for example in figure 5(c), we note that graphene increases the depth of binding energy well by as low as 5.85% (see S3 in supporting information) and therefore has very limited effect on the evaporation of a water molecule. This is significantly different from 'wetting transparency'. The wetting state involves the free energy of liquid water-substrate interface where both water-substrate and water–water interactions contribute, while only single water desorption energy (resulted from water-substrate interaction only) is relevant for evaporation.

Conclusion

The presence of graphene coating increases contact angle on hydrophilic substrates, while decreases contact angle on PDMS, which is in agreement with previous reports. Consequently, graphene decelerates the evaporation rate of droplet on hydrophilic substrates but accelerates evaporation rate on PDMS.

However, graphene has negligible effect on evaporation rate per contact line length, suggesting that graphene is transparent for evaporation at the contact line. MD simulations show the dynamics of water molecules at the contact line and unveil at molecular scale that predominant evaporation takes place as single water desorption at the contact line, because maximum transition state occurs at the line and decreases in the exponential form. Effects of graphene on the overall evaporation rate of droplet result from the fact that graphene changes the wetting states and contact line. Our findings reveal that molecule-level dynamics affect macroscopic evaporation process, and shed light on the atomistic mechanism and rational control of droplet evaporation on a solid substrate for various applications.

Methods

Sample preparation

We purchase STO and GaP from Hefei Kejing Materials Tech CO. LTD, glass from Jiangsu Fanchuan and Si from Anhui Institute of Optics and Fine Mechanics. PDMS mixing with curing agent at a volume ratio of 10:1 is spincoated on copper and then cured at 150 °C for 10 min. All the samples are washed in water, acetone, isopropanol and water by ultrasonic cleaner. Washing in every liquid lasts for 5 min. Samples after washing are dried by nitrogen blow.

Contact angle and evaporation measurements

Experimental setup is shown in Supporting Information. A digital balance (TS124S, Sartorius) with resolution of 0.1 mg is used to record real-time mass. At the same time we employ charge coupled device (Southern Vision Systems Inc) and Canon camera to take side-view photos of droplet profiles. OCA 20 (Dataphysics, Germany) is applied for both contact angle and contact diameter measurements. Droplet, generated by OCA 20, is gently placed on substrate and then put into the chamber with the size of 14 cm × 17 cm × 22 cm. A homebuilt setup above the droplet is used as a reference to measure contact diameter.

MD simulations

We adopt a model Si (100) substrate containing 26 377 atoms and gr/Si substrate containing 42 505 atoms in our simulations. Single-layer graphene is placed at a height of 0.34 nm above the Si surface. Cubic water box with the size of 4 nm × 4 nm × 4 nm containing 2109 water molecules is placed 0.5 nm above the substrate. Dimension of the system is 20.672 nm × 20.672 nm × 20 nm. Cutoffs for van der Waals interactions and electrostatic interactions within Ewald summation method are 1 nm [55]. In the first stage of simulation, the cubic water box is placed above substrate and then relaxed to equilibrium state at 300 K for 5 ns. In the second stage, the system is warmed to 330 K for evaporation. In this stage, the wall is placed in the upper boundary of the simulation cell with a cutoff of 14 nm, forming an absorption region. If a water molecule enters this region, it will be absorbed. The Lennard–Jones parameters for Si atom are $\sigma_{Si} = 0.5500$ nm and $\varepsilon_{Si} = 1.2000$ kJ mol^{-1}, for C atom $\sigma_C = 0.2500$ nm and $\varepsilon_C = 0.2300$ kJ mol^{-1}, for O atom $\sigma_O = 0.3151$ nm and $\varepsilon_O = 0.6364$ kJ mol^{-1} and for H atom $\sigma_H = 0.0400$ nm and $\varepsilon_H = 0.1925$ kJ mol^{-1} [54], respectively. TIP3P water model [55] is used to calculate water–water coulomb interactions with O-atom possessing $-0.834e$ and H-atom possessing $+0.417e$ as used previously [47, 52, 53]. Time step for evaporation is 1 fs and the simulation runs for at least 6 ns.

Acknowledgments

We acknowledge financial support from Ministry of Science and Technology (grant 2016YFA0300902), the National Natural Science Foundation of China (grants 11474328 and 11290164) and water project of Chinese Academy of Sciences. We are also grateful to Hao Wang for graphene transfer, Wenbin Zhang for building of experimental setup, Jingchuan Wang for data analysis and Cheng Yang for MD simulations.

ORCID iDs

Yongfeng Huang https://orcid.org/0000-0001-5185-491X
Sheng Meng https://orcid.org/0000-0002-1553-1432

References

[1] Deegan R, Dupont T, Huber G, Nagel S and Witten T 1997 *Nature* **389** 827–9
[2] Kim J, Kim J and Zin W 2007 *Langmuir* **23** 6163–9
[3] Kang S H, Wu N, Grinthal A and Aizenberg J 2011 *Phys. Rev. Lett.* **107** 177802
[4] Dugas V, Broutin J and Souteyrand E 2005 *Langmuir* **21** 9130–6
[5] Pinto P, Rosado C, Parreirao C and Rodrigues L M 2011 *Skin Res. Technol.* **17** 181–5
[6] Hof A and Wolf N 2014 *Landsc. Urban Plan* **123** 61–72
[7] Cira N J, Benusiglio A and Prakash M 2015 *Nature* **519** 446–50
[8] Xue G *et al* 2017 *Nat. Nanotechnol.* **12** 317–21
[9] Keiser L, Bense H, Colinet P, Bico J and Reyssat E 2017 *Phys. Rev. Lett.* **118** 074504
[10] Bachhuber C 1983 *Am. J. Phys.* **51** 259–64
[11] Chen X, Goodnight D, Gao Z, Cavusoglu A, Sabharwal N, DeLay M, Driks A and Sahin O 2015 *Nat. Commun.* **6** 7346
[12] Duan F, Badam V, Durst F and Ward C 2005 *Phys. Rev.* E **72** 056303
[13] Picknett R and Bexon R 1977 *J. Colloid Interface Sci.* **61** 336–50
[14] Birdi S and Winter A 1989 *J. Phys. Chem.* **93** 3702
[15] McHale G, Rowan S, Newton M and Banerjee M 1998 *J. Phys. Chem.* B **102** 1964–7
[16] Hu H and Larson R 2002 *J. Phys. Chem.* B **106** 1334–44
[17] Crafton E and Black W 2004 *Int. J. Heat Mass Tranfer* **47** 1187–200
[18] Anantharaju N, Panchagnula M and Neti S 2009 *J. Colloid Interface Sci.* **337** 176–82
[19] Chhasatia V, Joshi A and Sun Y 2010 *Appl. Phys. Lett.* **97** 231909
[20] Kelly-Zion P, Pursell C, Vaidya S and Batra J 2011 *Colloid Surf.* A **381** 31–6

[21] Yu Y, Wang Z and Zhao Y 2012 *J. Colloid Interface Sci.* **365** 254–9
[22] Shahidzadeh-Bonn N, Rafaï S, Azouni A and Bonn D 2006 *J. Fluid Mech.* **549** 307–13
[23] Gelderblom H, Bloemen O and Snoeijer J 2012 *J. Fluid Mech.* **709** 69–84
[24] Bones D, Reid J, Lienhard D and Krieger U 2012 *Proc. Natl Acad. Sci. USA* **109** 11613–8
[25] Penman H 1948 *Proc. R. Soc.* **193** 120–45
[26] Chuang Y, Chu C, Lin S and Chen L 2014 *Soft Matter* **10** 3394–403
[27] Dash S and Garimella S 2014 *Phys. Rev.* E **89** 042402
[28] Chen X, Weibel J and Garimella S 2015 *Sci. Rep.* **5** 17110
[29] Nascimento R, Cottin-Bizonne C, Pirat C and Ramos S M 2016 *Langmuir* **32** 2005–9
[30] Hens A, Biswas G and De S 2015 *J. Chem. Phys.* **143** 094702
[31] Sharma S and Debenedetti P 2012 *Proc. Natl Acad. Sci. USA* **109** 4365–70
[32] Roger K, Liebi M, Heimdal J, Pham Q and Sparr E 2016 *Proc. Natl Acad. Sci. USA* **113** 10275–80
[33] Chen X, Ma R, Li J, Hao C, Guo W, Luk B L, Li S C, Yao S and Wang Z 2012 *Phys. Rev. Lett.* **109** 116101
[34] Chen X and Wang Z 2015 *J. Heat Transfer* **137** 080903
[35] Miljkovic N, Preston D, Enright R and Wang E 2013 *ACS Nano* **7** 11043–54
[36] Novoselov K, Geim A, Morozov S, Jiang D, Zhang Y, Dubonos S, Grigorieva I and Firsov A 2004 *Science* **306** 666–9
[37] Geim A and Novoselov K 2007 *Nat. Mater.* **6** 183–91
[38] Geim A 2009 *Science* **324** 1530–4
[39] Rafiee J, Mi X, Gullapalli H, Thomas A, Yavari F, Shi Y, Ajayan P and Koratkar N 2012 *Nat. Mater.* **11** 217–22
[40] Raj R, Maroo S and Wang E 2013 *Nano Lett.* **13** 1509–15
[41] Shih C, Wang Q, Lin S, Park K, Jin Z, Strano M and Blankschtein D 2012 *Phys. Rev. Lett.* **109** 176101
[42] Shih C, Wang Q, Lin S, Park K, Jin Z, Strano M and Blankschtein D 2015 *Phys. Rev. Lett.* **115** 049901
[43] Li Z *et al* 2013 *Nat. Mater.* **12** 925–31
[44] Wang Y, Zheng Y, Xu X, Dubuisson E, Bao Q, Lu J and Loh K 2011 *ACS Nano* **5** 9927–31
[45] Gao L *et al* 2012 *Nat. Commun.* **3** 699
[46] Ferrari A *et al* 2006 *Phys. Rev. Lett.* **97** 187401
[47] Mason P 2011 *J. Phys. Chem.* A **115** 6054–8
[48] Varilly P and Chandler D 2013 *J. Phys. Chem.* B **117** 1419–28
[49] Wang F and Wu H 2013 *Soft Matter* **9** 5703–9
[50] Nagata Y, Usui K and Bonn M 2015 *Phys. Rev. Lett.* **115** 236102
[51] Plimpton S 1995 *J. Comput. Phys.* **117** 1–19
[52] Wang S, Tu Y, Wan R and Fang H 2012 *J. Phys. Chem.* B **116** 13863–7
[53] Wan R, Wang C, Lei X, Zhou G and Fang H 2015 *Phys. Rev. Lett.* **115** 195901
[54] Bjelkmar P, Larsson P, Cuendet M, Hess B and Linal E 2010 *J. Chem. Theory Comput.* **6** 459
[55] Jorgensen W, Chandrasekhar J, Madura J, Impey R and Klein M 1983 *J. Chem. Phys.* **79** 926–35